

The design and optimization of the mixing process for Udimet 720LI nickel alloy manufacturing from elemental powders

Wiktoria Skonieczna^{1*} , Marek Wojtaszek¹ , Oleksandr Lypchanskyi¹ ,
Kamil Cichocki¹ , Marcin Goły¹ , Mateusz Kopyściański¹ , Dariusz Zientara² ,
Rafał Stanik³ , Maik Gude³ , Ulrich Prah⁴ 

¹ Faculty of Metals Engineering and Industrial Computer Science, AGH University of Krakow, al. Adama Mickiewicza 30, Krakow, Poland

² Faculty of Materials Science and Ceramics, AGH University of Krakow, al. Adama Mickiewicza 30, Krakow, Poland

³ Institute of Lightweight Engineering and Polymer Technology (ILK), Technische Universität Dresden, Holbeinstr. 3, 01307 Dresden, Germany

⁴ Institute of Metal Forming, Technische Universität Bergakademie Freiberg, Bernhard von Cotta Strasse 4, 09599 Freiberg, Germany

* Corresponding author's e-mail: skoniecz@agh.edu.pl

ABSTRACT

The objective of the study was to design an efficient production route for the U720LI nickel alloy using elemental powders as initial materials. The powder mixing process was carried out using a double-cone mixer and an Attritor mill, respectively. A device proper for effective mixing and mechanical alloying of powder particles was selected, and the most favorable parameters for the powder mixing process necessary for the production of the alloy were developed. The analysis of the results showed that significantly higher efficiency in mixing the powders necessary for producing the U720LI alloy was achieved using the Attritor mill. In further tests, the most favorable operating parameters of this device were determined by mixing materials at different rotational speeds. The results demonstrated that the most effective method of powder bonding among the tested variants was mixing in the Attritor mill at the identified high rotational speeds. A highly densified product with a homogeneous microstructure and free of external and internal defects was obtained, suitable for use both as a finished product and as high-quality feedstock for hot metal forming processing.

Keywords: nickel superalloys, powder metallurgy, powder mixing, mechanical alloying, elemental powders, SEM.

INTRODUCTION

Nickel alloys represent a unique group of structural materials characterized by an exceptionally high set of material properties. They are primarily known for their excellent resistance to high-temperature corrosion [1] and oxidation [2]. Additionally, these materials exhibit high fatigue [3] and creep resistance [4]. The combination of these properties makes nickel alloys practically indispensable in many applications, particularly in critical structural components used in the

aerospace industry, such as those operating in the high-temperature zones of engines [5, 6]. These alloys are also used in various other applications, including components for solar panels [7], energy storage containers [8], and parts working in gas turbines [9]. The widespread use of nickel-based alloys and their highly demanding applications impose stringent requirements, typically associated with rigorous production and acceptance conditions. This factor results in production costs that are above average compared to other structural materials, partly due to the very challenging

machining of these alloys [10]. The production of nickel-based alloys involves numerous technological [11] and economic challenges, requiring specialized knowledge and the implementation of advanced technical solutions. Ensuring the purity of raw materials [12] and precise control of the chemical composition of alloys are among the key issues directly affecting the properties of the materials [13]. Moreover, apart from technological aspects, economic considerations related to optimizing production costs and minimizing environmental pollution are also significant. This is because the production of nickel alloys is often energy-intensive and leads to CO₂ emissions, with the manufacturing processes generating waste that must be properly managed to meet high environmental standards [14]. In response to these challenges, the nickel metallurgy industry seeks innovative solutions that offer the potential for developing more efficient production processes or adopting technologies that reduce energy consumption and greenhouse gas emissions.

One of the approaches in nickel alloy manufacturing is the implementation of powder metallurgy technologies into the production chain. A considerable group of nickel alloys, produced directly from powders, has already been developed and found applications in the aerospace industry, including alloys from the Rene and FGH [15] families. Furthermore, researchers are also attempting to develop comprehensive technologies for producing conventional casting alloys through alternative methods based on powder metallurgy [16]. However, most of the production routes developed to date use expensive master powders [17] as starting materials and employ the Hot Isostatic Pressing (HIP) technology, which requires costly and complex equipment [18]. A fundamental reason for this approach is that it ensures a uniform microstructure and properties throughout the volume of the products, which is crucial. When using elemental powders as starting materials and attempting to consolidate them with alternative technologies, meeting these requirements poses a significant research challenge.

Udimet 720 (U720LI) belongs to the group of nickel superalloys. This material is a typical casting alloy, which is usually further shaped through plastic deformation [19]. Currently, it is mainly used for the production of discs and blades in aircraft engine turbines [20]. Additionally, due to its high mechanical properties at elevated temperatures, such as creep resistance, fatigue

resistance, as well as high-temperature corrosion and oxidation resistance, this alloy is also used as a material for gas turbine components [21]. Its mechanical properties are primarily dependent on the microstructure [22], which can be controlled through the selection of appropriate hot deformation parameters, such as temperature, strain rate, and deformation rate [23]. Before the deformation process, ingots of U720LI alloy are usually subjected to homogenization at a temperature of approximately 1160 °C. However, the duration of this process can last up to 50 hours, further increasing the process costs [24]. Another limitation is the wear of heating installations, which are typically designed for shorter heat treatment processes. The time-consuming and costly high-temperature homogenization of U720LI alloy can be addressed by producing this material using powder metallurgy-based technology, which promotes achieving a more uniform microstructure than is possible in conventional casting processes [25]. By utilizing relatively inexpensive elemental powders in the production process and applying hot pressing sintering as a consolidation method, production costs can be reduced. However, this approach requires consideration of the critical factor of ensuring proper powder mixing, which guarantees uniform distribution throughout the mixture. Failing to meet this condition excludes the possibility of producing high-quality products from such a mixture [26], regardless of the subsequent processing method. In the case of U720LI alloy, due to the stringent requirements imposed on this material, achieving a homogeneous mixture requires precise design of this production stage.

Numerous researchers have investigated the fabrication of high-quality alloys using elemental powders. To achieve this, a diverse array of methods has been employed, including blending in a double-cone mixer followed by cold pressing and free sintering [27], or utilizing hot pressing as an alternative consolidation technique [28], which ensures a high relative density. Additionally, the literature highlights approaches where high-energy ball milling [29] is used to prepare powder mixtures. These mixtures are subsequently subjected to compaction and hot sintering, similar to the DCB mixing process, or undergo more advanced densification techniques such as electric field-assisted hot-pressing sintering [30]. Another key element is the selection of a manufacturing technology for the mixture that ensures the production of a defect-free

product with a high relative, a favorable microstructure, and sufficiently high properties. Additionally, the proposed technology should be cost-competitive. These challenges and the difficulties in addressing them are likely the reason why such an approach for U720LI alloy has not yet been developed or extensively described in the literature. The lack of available knowledge relates to both the methods and parameters of the processes for producing and consolidating the mixture, as well as information on the impact of these process parameters on the quality, microstructure, and properties of the product. Developing this data is considered by the authors as an interesting scientific challenge, offering potential for practical application due to the technological and economic benefits of using elemental powders and a consolidation method competitive to HIP. This consideration motivated the authors to undertake the issue and carry out the research presented in this study. The primary objective of this research was to develop a new, efficient, and economical production route for the U720LI nickel superalloy using elemental powders.

EXPERIMENTAL METHODS

Elemental powders of nickel, cobalt, chromium, titanium, aluminum, and molybdenum were used as the initial materials. These powders

were employed in proportions corresponding to the nominal composition of the U720LI alloy, as listed in Table 1. The morphology of elemental powders was evaluated using a Hitachi TM-3000 scanning electron microscope. The appropriately weighed powders were subjected to processes of mixing, and mechanical alloying in devices with significantly different operating characteristics: a double-cone blender and an Attritor mill. The use of two distinct devices aimed to identify the more effective mixing method that would economically produce a homogeneous mixture, considered essential for subsequently producing a high-quality alloy.

The method chosen for consolidating the mixture into an alloy involved hot compacting. The technological routes selected for the production of the U720LI alloy are presented in Figure 1. The quality of the mixtures and, based on this, the evaluation of the effectiveness of the mixing process by the respective methods and parameters were assessed using X-ray diffraction (XRD) analysis performed on a Simens D500 diffractometer, as well as scanning electron microscopy (SEM) and energy dispersive spectroscopy (EDS) studies conducted with an FEI Nova Nano SEM scanning electron microscope.

The production of the U720LI alloy from the mixture prepared using the developed technology was carried out through hot compacting on a

Table 1. Chemical composition of manufactured alloy

Element	Ni	Co	Cr	Ti	Mo	Al	W
Wt. %	Bal.	14.9	14.7	4.0	2.6	2.4	1.3

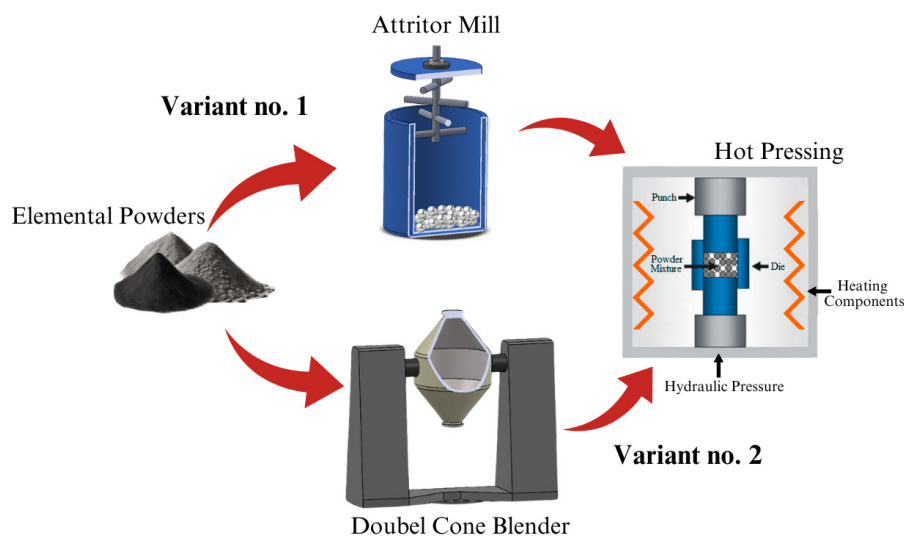


Figure 1. Diagram of the designed technological process for U720LI alloy production

Thermal Technology Press Inc. machine, capable of processing at temperatures up to 1600 °C in an argon protective atmosphere. The assessment of the compact quality included non-destructive testing of the material’s internal structure using computed tomography (CT), determination of relative density by the Archimedes method, microstructure analysis using SEM and electron backscatter diffraction (EBSD) methods, and hardness measurements using the Vickers method. The CT test was performed with a v|tome|x L-450 tomograph with a maximum resolution of 1 μm. SEM and EBSD analyses were conducted using a ZEISS GeminiSEM 450 microscope. The preparation of material for electron microscopy analysis involved selecting a representative region of the material and cutting it using a specialized metallographic saw. The extracted material specimen was embedded in conductive PolyFast resin, followed by grinding with abrasive papers ranging from P500 to P1200 according to the FEPA scale. Subsequently, the cross-section was polished on specialized polishing cloths using diamond suspensions with particle sizes ranging from 9 μm to 1 μm. The final step of material preparation involved additional polishing utilizing an OP-S suspension. Hardness measurements

of the sinter were performed on a Druramin-40 hardness tester by Struers, with a load of 10 kgf applied during testing.

RESULTS AND DISCUSSION

Initial material

Observations of the individual powder particles necessary for producing the U720LI alloy were conducted using a method of scanning electron microscopy. The morphology of the powder particles is presented in Fig. 2.

The shape and average size of the elemental powder particles used as starting materials varied due to the different production methods employed by manufacturers. The particle sizes ranged from 3 μm to 150 μm. A spherical shape and smooth surface were characteristic features of powders produced by atomization, such as aluminum. Irregular shapes and rough surfaces were typical of powders obtained through reduction processes (chromium, cobalt, molybdenum, tungsten) or HDH technology (titanium). The spherical nickel powder was obtained through the carbonyl process.

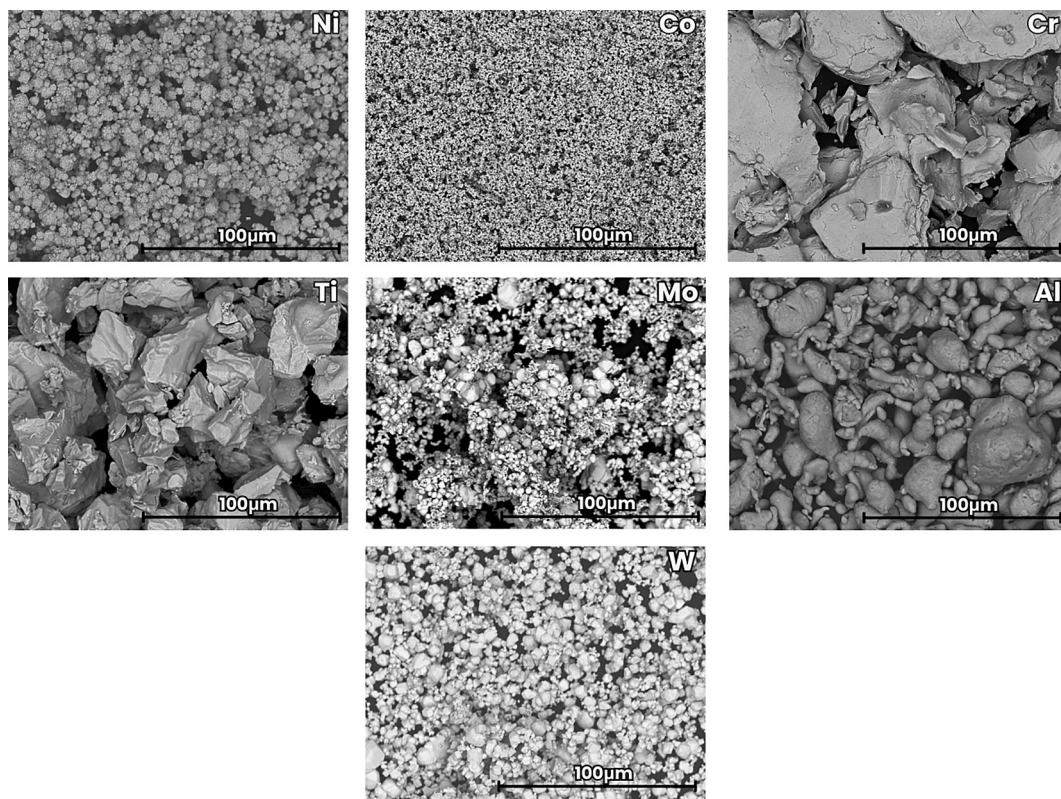


Figure 2. Morphology of elemental powder particles used in the research

Mixing process

To conduct the mixing process of elemental powders, two devices were initially selected: a double-cone blender (DCB) and a high-energy attritor mill (MA). In the DCB, the mixing operation was performed in small ceramic crucibles, each capable of holding 90 grams of powder along with tungsten carbide balls, with a ball-to-powder weight ratio (BPR) of 7:1. The introduction of balls into the system aimed to intensify the mixing process and achieve the mechanical bonding of particles. A mixing time of 180 minutes was established. The process was conducted at the maximum rotational speed of the blender, set at 55 rpm. The Attritor mill allowed for the simultaneous mixing of larger quantities of powder due to the larger capacity of its chamber. A total of 250 grams of powder was introduced into the container along with steel balls, with a BPR of 12:1. Milling in the Attritor was also conducted for 180 minutes, at a stirrer speed of 250 rpm. Additionally, the Attritor enabled the process to be conducted in a protective atmosphere of inert gas to prevent intense oxidation of the mixture, using argon for this purpose. After the mixing process, a sample of material from each batch was taken for XRD analysis. The XRD analysis results are presented in Figures 3 for comparison, an additional XRD analysis was performed on the powders initially loaded into the chamber and manually pre-mixed (state 0), which is prior to the commencement of the actual mixing process in the devices.

The analysis and comparison of the XRD diffractograms clearly indicated a significantly

higher efficiency of the Attritor mill method compared to the outcomes obtained using the DCB. Comparing the XRD patterns, a notable reduction in peak intensities for individual elements within the mixtures was observed for the material mixed using the Attritor method. Specifically, the largest peak corresponding to nickel showed an almost fivefold decrease in intensity for the mixture processed with the Attritor, compared to the peak intensity of the mixture obtained via the DCB process. Additionally, the mixture produced in the DCB was only marginally better homogenized than the initial state, reflecting the low efficiency of this method. Furthermore, SEM observations (Fig. 4) combined with EDS analysis (Fig. 5) of the produced mixtures were conducted. These studies allowed for the characterization of particle morphology in the mixtures and provided a more detailed assessment of the efficiency of the mixing processes.

The mixture produced using the DCB method (Fig. 4a) is characterized by particles of varying sizes and shapes. Very large particles are observed alongside particles of significantly smaller sizes. Furthermore, the morphology of the DCB mixture still allows for the identification of individual elemental powder particles, as their shape did not undergo significant changes during the mixing process. In contrast, the powder particles obtained using the MA method (Fig. 4b), despite their larger size, are relatively uniform in shape and do not differ significantly from each other. Their shape and size result from the effects of intense particle impaction, fragmentation, and

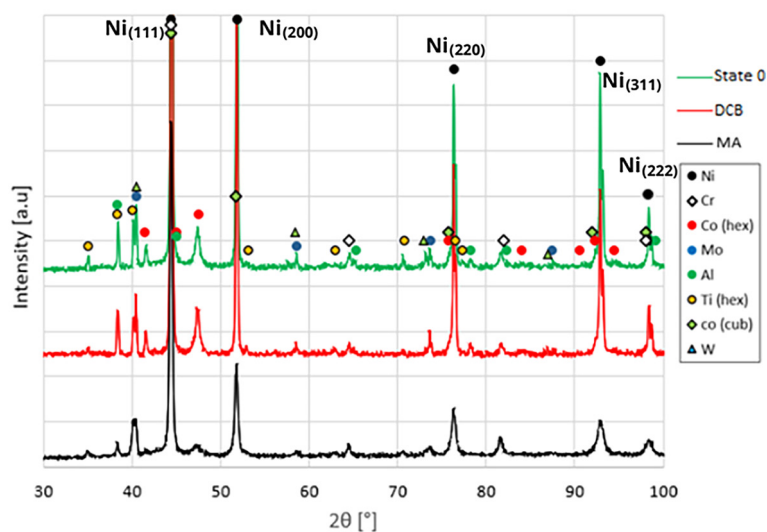


Figure 3. Results of XRD analysis conducted for tested powder mixtures

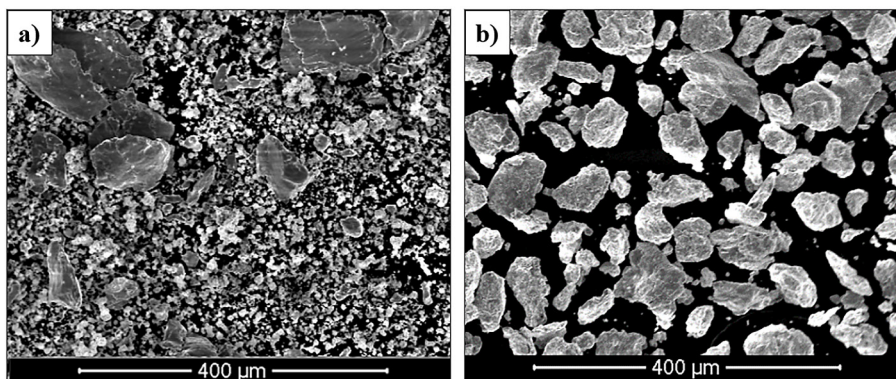


Figure 4. Micrographs of mixtures produced in the devices: (a) DCB, (b) MA

mechanical bonding. Compared to the DCB mixture, individual particles in the MA mixture cannot be identified as components of specific starting powders. The comparable particle size suggests that these processes occurred simultaneously and uniformly throughout the entire volume of the mixture during the process.

The EDS analysis confirmed the conclusions drawn from SEM observations of the tested mixtures. The EDS examination of the mixture produced using the DCB method (Fig. 5a) revealed a clear separation of individual elemental powders, indicating low efficiency of the mixing process. The particles in the mixture produced by the MA process (Fig. 5b) are more uniform in both size and shape. The particles resulting from this process do not exhibit the morphological characteristics of the original elements. This indicates that during the mixing process, high energy led to the alternating welding of individual particles into larger agglomerates, followed by subsequent crushing or breaking of the formed clusters. This phenomenon, known in the literature as mechanical alloying, resulted in the creation of entirely new powder particles, whose chemical composition throughout their

volume aligns with that required for the production of the nickel U720LI alloy.

The conducted studies and the analysis of the obtained results clearly demonstrated a significantly greater efficiency of mixing using the Attritor mill, leading to the rejection of the DCB method at this stage.

Mixing parameters optimization

During the efficiency tests of the equipment, the initial operating parameters of the mill were selected based on available literature related to mechanical alloying technology. The initial setup focused on determining an optimal ball-to-powder weight ratio, which was ultimately set at 12:1. This BPR was chosen to maximize the amount of powder while ensuring that the quantity of balls was sufficient to induce phenomena that intensify the mechanical alloying process. A similar BPR was used by Dymek et al. in their studies on a niobium alloy [31], where mechanical alloying was conducted using an Attritor mill.

A critical factor was the rotational speed of the powder mixing process, which in the first trial

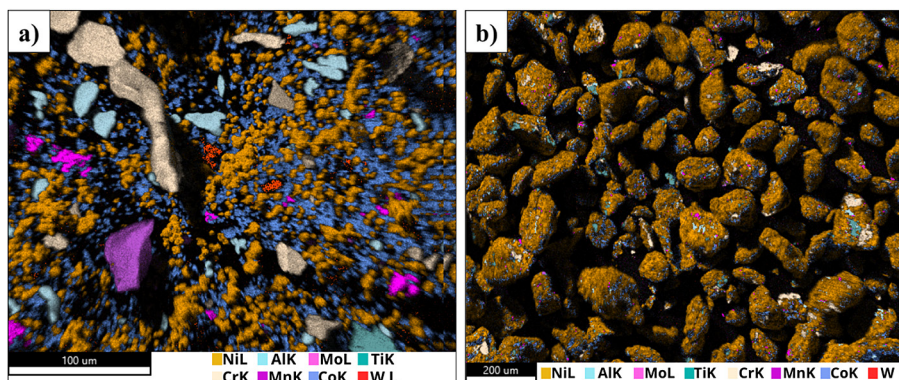


Figure 5. EDS analysis results of mixtures produced in the devices: (a) DCB, (b) MA

was set at 250 RPM. The choice of this speed was influenced by the findings of [32], which described the production of nickel alloy powder using mechanical alloying in a planetary ball mill. However, further review of the literature on the subject revealed additional sources where higher mixing speeds were employed for materials with a face-centered cubic (FCC) structure [33, 34]. Consequently, additional tests were conducted at mixing speeds of 300 RPM and 350 RPM (the maximum operating range of the equipment). For these tests, the XRD and SEM analyses of the mixtures were performed, following the same methodology as in the comparative efficiency tests of the equipment.

The diffractograms obtained for the mixtures processed at higher rotational speeds (Fig. 6) show a tendency for a reduction in the intensity of peaks corresponding to individual phases/elements, accompanied by peak broadening. This indicates that increasing the rotational speed of mixing enhances the material homogenization while simultaneously reducing the crystallite size. The best homogenization results were achieved at a mixing speed of 350 RPM. In this variant, the intensity of the highest peak corresponding to the nickel signal decreased by nearly half compared to the results obtained at 300 RPM.

In addition, based on the results obtained, the size of the crystallites of the test material was also calculated. The obtained crystallite sizes were as follows: 8.69 μm for milling at 250 RPM, 7.96 μm for milling at 300 RPM, and 7.06 μm for milling at 350 RPM. The analysis of crystallite size variation in tested powders reveals a decrease in

crystallite size with an increase in the rotational speed of the milling apparatus. This trend can be attributed to the intensified mechanical energy input, which enhances the fragmentation and refinement of crystalline structures. Higher rotational speeds generate greater shear forces and collision impacts, leading to more efficient grain boundary formation and reduction of crystallite size. Moreover, the results demonstrate very high correlation coefficient of 0.99, indicating that the crystallite size reduction is consistently proportional to the milling speed.

Observations of the particles in mixtures produced at rotational speeds of 300 RPM (Fig. 7a) and 350 RPM (Fig. 7b) reveal no significant differences in particle morphology. Additionally, the size of the particles obtained in both cases is fairly uniform and comparable. However, it was noted that the average particle size is larger than that observed in the mixture produced in the mill at 250 RPM.

Taking into account the information gathered from the preliminary analysis of the literature on mechanical alloying technology, the results of the conducted research on this technology concerning the applied elemental powders, and considering the technological possibilities and limitations (e.g., the maximum rotational speed of the Attritor mill), the most advantageous process for achieving effective mixing and bonding of the input powders necessary to produce the U720LI alloy was identified as the MA process in the Attritor mill. This process is conducted for 180 minutes, at a rotational speed of 350 RPM, with a BPR of 12:1.

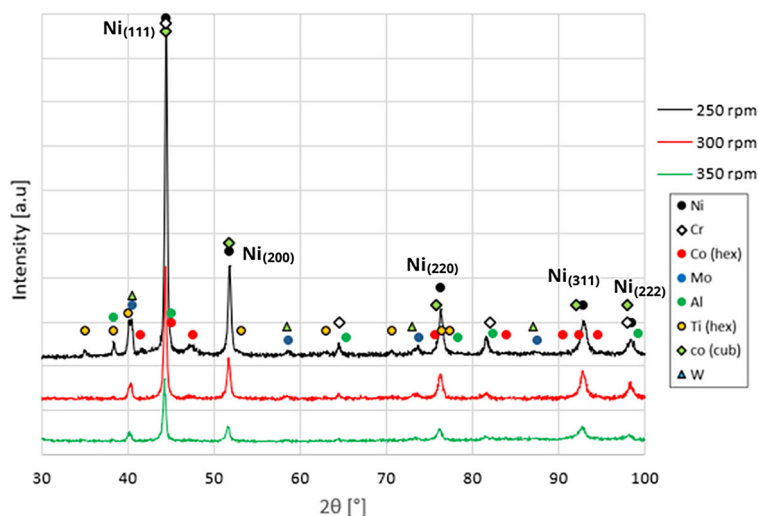


Figure 6. XRD analysis results for mixtures obtained in the attritor mill at different mixing speeds

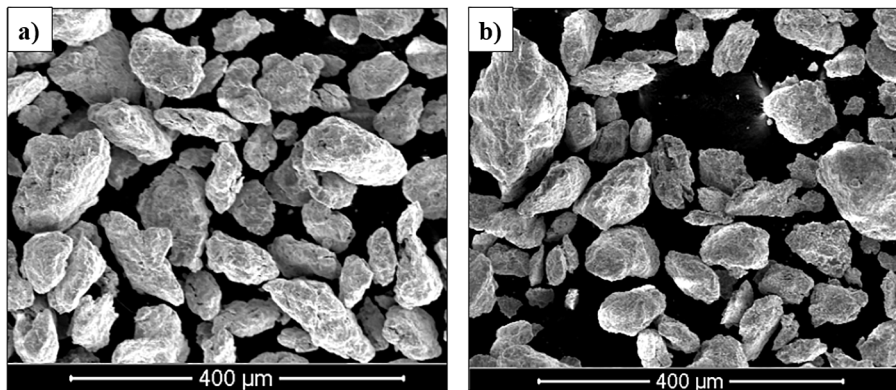


Figure 7. Micrographs of mixtures produced in the Attritor mill at mixing speeds of: (a) 300 RPM, (b) 350 RPM

Powder consolidation

To verify the correctness of the developed method and parameters for preparing the elemental powder mixture, the consolidation process was carried out using hot compaction process. The process was conducted in graphite molds at a temperature of 1200 °C, with an applied pressure of 25 MPa, maintained for 2 hours. To prevent oxidation, sintering was performed in a protective argon atmosphere. The result was a cylindrical compact with a diameter of 77 mm and a height of 44 mm, free from visible external defects.

To confirm the quality of the sinter produced under the established conditions, the material underwent non-destructive internal structure testing using CT. The compact was scanned using a

resolution of 50 μm. The results of the CT observations (Fig. 8) confirmed that the material produced is free from cracks and other internal defects, such as discontinuities or delaminations. Additionally, the analysis of the tomographic scans did not reveal pores or other voids exceeding the resolution limit of the tests.

To confirm the CT scan results and to perform a quantitative assessment of porosity, the relative density of the compact was measured using the Archimedes method. The compact was found to have a relative density exceeding $98.67 \pm 0.84\%$.

Subsequently, the microstructure of the compact was evaluated through SEM observations and EBSD analysis.

The microstructure of the hot compacted material (Fig. 9) is characterized by a typical FCC

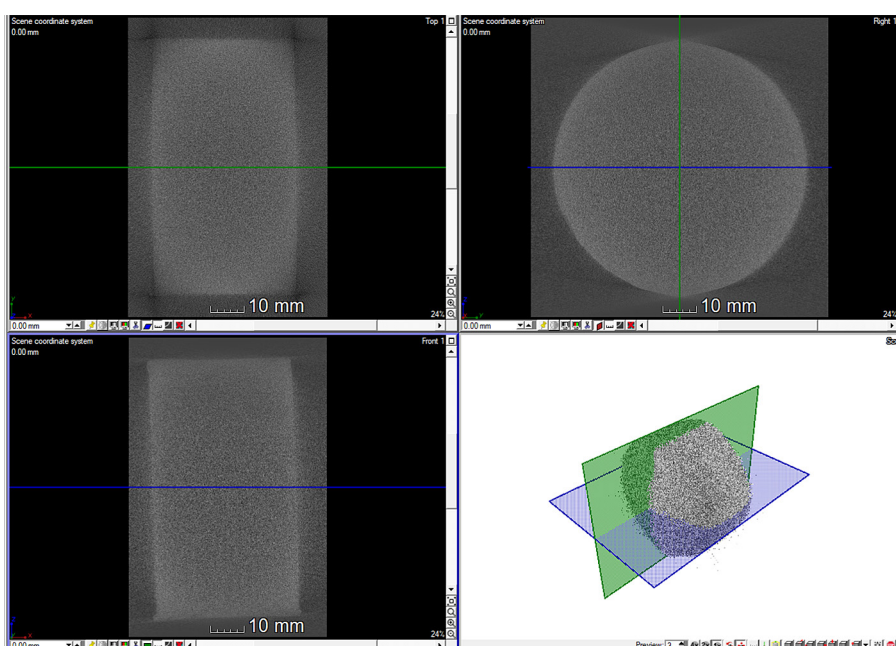


Figure 8. Results of CT non – destructive test performed on the U720LI compact

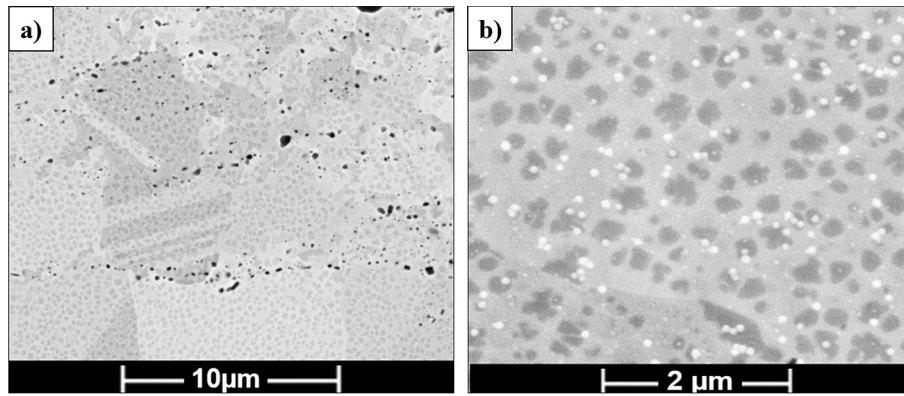


Figure 9. Microstructure of the hot-pressed sample obtained via SEM imaging with lower (a) and higher (b) magnification

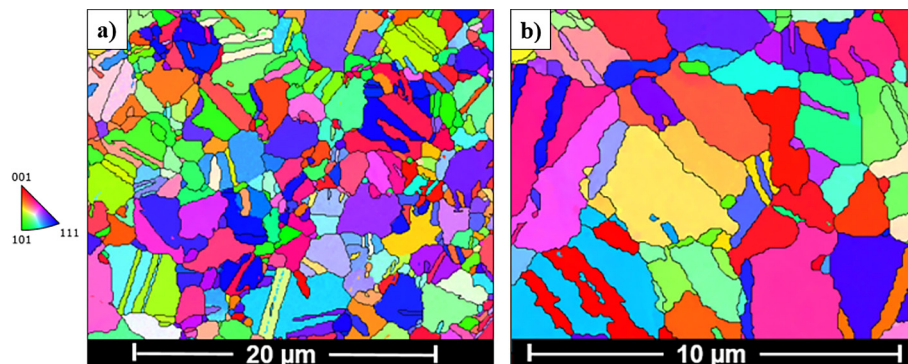


Figure 10. Microstructure of the sintered material in reference to EBSD IPF maps with lower (a) and higher (b) magnification

austenitic structure with distinctive twin boundaries. SEM micrographs obtained at higher magnifications revealed the presence of relatively uniformly distributed the γ' phase, $\text{Ni}_3(\text{Al}, \text{Ti})$ in the structure. This phase plays a crucial role in the material's microstructure and its properties. These finely dispersed, coherent precipitates within the γ matrix create significant barriers to dislocation movement, enhancing strength through precipitation hardening.

The EBSD maps presented in Figure 10 provided additional insights into the microstructural state of the material, such as grain crystallographic orientation, and facilitated the identification of individual grain boundaries. The estimated average grain size in the produced material was approximately $18 \mu\text{m}$.

Additionally, Vickers hardness measurements were conducted using a 10 kgf load, performed with a Druramin-40 hardness tester from Struers. The average hardness of the material, measured from 16 readings, was $447 \pm 6 \text{HV}_{10}$. The obtained high hardness of the material is directly related to

the presence of γ' phase precipitates ($\text{Ni}_3(\text{Al}, \text{Ti})$). Its uniform distribution and significant volume fraction in the structure affect the high resistance of the material against the indenter force.

CONCLUSIONS

Based on the results of the research aimed at designing an efficient mixing process for production route of the U720LI nickel alloy from elemental powders, it was concluded that:

The appropriate selection of powder mixing techniques and their operational parameters is crucial for achieving material homogenization. The XRD studies revealed significant differences in the uniformity of the obtained mixtures depending on the device used. With the same mixing time, the Attritor mill achieved significantly higher particle mixing efficiency compared to the double-cone mixer.

SEM analysis of the mixture produced in the double-cone mixer allowed for the identification

of individual powder particles due to the inefficient mixing effect. In the mixture obtained using the Attritor mill, changes in particle sizes and shapes were observed, with particles showing no distinct characteristics of the original powders and forming conglomerates.

EDS analysis revealed a very uniform distribution of elements within the volume of the mixture produced using the MA method. In contrast, the DCB method resulted in uneven distribution of individual powder particles, with areas of strong concentration or absence of particles of a particular element.

Increasing the mixing speed of the powders led to an improvement in the homogenization of the mixture produced using the MA method. The best material homogenization was achieved at a mixing speed of 350 RPM.

The hot compaction of the mixture produced using the developed method was successful, achieving a material free of internal defects and with a relative density above 99%. The compact microstructure is uniform with a fine grain size, averaging 18 μm . The average hardness of the compact is relatively high, measuring $447 \pm 6 \text{ HV}_{10}$.

The obtained results indicate that the developed material can be competitive with alloys of the same chemical composition produced using conventional manufacturing methods, demonstrating the potential application of the developed production route for U720LI alloy. However, comprehensive testing of the produced compact properties and the development of process parameters for its formation in hot deformation processes are necessary for confirmation.

Acknowledgements

The research was carried out with the financial support of the Polish Ministry of Science and Higher Education form AGH-UST Statutory Research Project No. 16.16.110.663-operation 7.

REFERENCES

1. Wenga T., Gwenzi W., Jamro I.A., Ma W. High-temperature corrosion-resistant alloy for waste-to-energy plants: Alloy designing, fabrication, and possible corrosion-resistance mechanism. *Heliyon*, 2024, 10, 9, e30177. <https://doi.org/10.1016/j.heliyon.2024.e30177>
2. Shen J., Sun W., Xie L. et. al. Achieving well-balanced mechanical properties and oxidation

- resistance of an oxide dispersion strengthened nickel-based alloy via in-situ solid-state reaction. *Ceram. Int.* 2024, 50, 13, 22514–22523. <https://doi.org/10.1016/j.ceramint.2024.03.353>
3. Xu J., Yuan H., Investigation of damage mechanisms in thermomechanical fatigue of nickel-based single-crystal alloys. *Eng. Fract. Mech.* 2024, 297, 109871. <https://doi.org/10.1016/j.engfracmech.2024.109871>
4. Tian N., Zhao G., Shi Z. et. al. High-temperature creep behaviour and deformation mechanism of a high-concentration Re/Ru single-crystal nickel-based alloy. *J. Mater. Res. Technol.* 2024, 29, 1350–1358. <https://doi.org/10.1016/j.jmrt.2024.01.131>
5. Wang S., He J., Li W. et. al. Microstructure analysis and cracking mechanism of aero-engine hot-end component K4169 superalloy based on in-situ EBSD test. *J. Alloys Compd.* 2023, 960, 70781. <https://doi.org/10.1016/j.jallcom.2023.170781>
6. Anand Kumar S., Rajkumar V. et. al. Single crystal metal deposition using laser additive manufacturing technology for repair of aero-engine components. *Mater. Today Proc.* 2021, 45, 6, 5395–5399. <https://doi.org/10.1016/j.matpr.2021.02.083>
7. Lambrecht M. et. al. Temperature dependence of high-temperature corrosion on nickel-based alloy in molten carbonates for concentrated solar power applications. *Corros. Sci.* 2023, 220, 111262. <https://doi.org/10.1016/j.corsci.2023.111262>
8. Nei J., Wang M. Hydrogen storage alloy development for wide operating temperature nickel-metal hydride battery applications. *Int. J. Hydrogen Energy* 2024, 49, 19–38. <https://doi.org/10.1016/j.ijhydene.2023.09.087>
9. Ashwin Prabhu G. et. al. Heat treatment and analysis of nickel super alloy for gas turbine applications. *Mater. Today Proc.* 2021, 39, 4, 1417–1421. <https://doi.org/10.1016/j.matpr.2020.05.098>
10. Pimenov D. Y. et. al. A comprehensive review of machinability of difficult-to-machine alloys with advanced lubricating and cooling techniques. *Tribol. Int.* 2024, 196, 109677. <https://doi.org/10.1016/j.triboint.2024.109677>
11. Darolia R. Development of strong, oxidation and corrosion resistant nickel-based superalloys: critical review of challenges, progress and prospects. *Int. Mater. Rev.* 2018, 64, 6, 355–380. <https://doi.org/10.1080/09506608.2018.1516713>
12. Meshram P., Abhilash, Pandey B. D. Advanced Review on Extraction of Nickel from Primary and Secondary Sources. *Miner. Process. Extr. Metall. Rev.* 2018, 40, 3, 157–193. <https://doi.org/10.1080/08827508.2018.1514300>
13. Ganji D.K., Rajyalakshmi G. Influence of alloying compositions on the properties of nickel-based

- superalloys: A review. *Recent Advances in Mechanical Engineering*, 2020, 537–555. https://doi.org/10.1007/978-981-15-1071-7_44
14. Wei W., Samuelsson P.B. et al. Energy consumption and greenhouse gas emissions of nickel products. *Energies* 2020, 13, 5664. <https://doi.org/10.3390/en13215664>
 15. Yang L., Ren X., et al. Status and development of powder metallurgy nickel-based disk superalloys. *Int. J. Mater. Res.* 2019, 110, 10, 901–910. <https://doi.org/10.3139/146.111820>
 16. Tian X., Wu J., Lu Z. et al. Effect of powder size segregation on the mechanical properties of hot isostatic pressing Inconel 718 alloys. *J. Mater. Res. Technol.* 2022, 21, 84–96. <https://doi.org/10.1016/j.jmrt.2022.09.009>
 17. Ye L., Liu F., et al. Investigation on the microstructure and mechanical properties of ni-based superalloy with scandium. *Metals* 2023, 3, 3. <https://doi.org/10.3390/met13030611>
 18. Sreenu B., Sarkar R., Satheesh Kumar S.S., et al. Microstructure and mechanical behaviour of an advanced powder metallurgy nickel base superalloy processed through hot isostatic pressing route for aerospace applications. *Mater. Sci. Eng. A* 2020, 797, 140254. <https://doi.org/10.1016/j.msea.2020.140254>
 19. Liu F., Chen J., Dong J., Zhang M., Yao Z. The hot deformation behaviors of coarse, fine and mixed grain for Udimet 720Li superalloy. *Mater. Sci. Eng. A* 2016, 651, 102–115. <https://doi.org/10.1016/j.msea.2015.10.099>
 20. Kumar D., Idapalapati S., Wei W. Microstructural Response and Strain Hardening in Deep Cold Rolled Nickel-based Superalloy for Aerospace Application. *Procedia CIRP* 2018, 71, 374–379. <https://doi.org/10.1016/j.procir.2018.05.044>
 21. Aba-Perea P.E., Pirling T. et al. Determination of the high temperature elastic properties and diffraction elastic constants of Ni-base superalloys. *Mater. Des.* 2016, 89, 856–863. <https://doi.org/10.1016/j.matdes.2015.09.152>
 22. Xie B.C., Ning Y.Q., Zhou C. Deformation behavior and microstructure evolution of two typical structures in Udimet 720Li ingot. *Procedia Eng.* 2017, 207, 1093–1098. <https://doi.org/10.1016/j.proeng.2017.10.1136>
 23. Wan Z., Hu L., Sun Y., Wang T., Li Z. Hot deformation behavior and processing workability of a Ni-based alloy. *J. Alloys Compd.* 2018, 769, 367–375, <https://doi.org/10.1016/j.jallcom.2018.08.010>
 24. Fan H., Jiang H., Dong J., Yao Z., Zhang M. An optimization method of upsetting process for homogenized, nickel-based superalloy Udimet 720Li ingot considering both cracking and recrystallization. *J. Mater. Process. Technol.* 2019, 269, 52–64. <https://doi.org/10.1016/j.jmatprotec.2019.01.013>
 25. Clement C., Panuganti S., Warren P. H. et al. Comparing structure-property evolution for PM-HIP and forged alloy 625 irradiated with neutrons to 1 dpa. *Mater. Sci. Eng. A* 2022, 857, 144058. <https://doi.org/10.1016/j.msea.2022.144058>
 26. Suryanarayana C. Mechanical alloying: a critical review. *Mater. Res. Lett.* 2022, 10, 10, 619–647. <https://doi.org/10.1080/21663831.2022.2075243>
 27. Zygula K., Lypchanskyi O., Cichocki K., et al. Achieving high density and controlled microstructure by predicting hot deformation behavior of low-cost powder metallurgy Ti-5553 alloy. *J. Mater. Res. Technol.* 33, 2024, 8403–8424. <https://doi.org/10.1016/j.jmrt.2024.11.180>
 28. Zygula K., Lypchanskyi O., Łukaszek-Solek A. et al. A Comprehensive Study on Hot Deformation Behavior of the Metastable β Titanium Alloy Prepared by Blended Elemental Powder Metallurgy Approach. *Metall. Mater. Trans. A* 2024 55, 933–954. <https://doi.org/10.1007/s11661-024-07297-9>
 29. Niu B., Liu Q., et al. Influence of powder ball milling pretreatment on microstructure and properties of Mo-W-Cu refractory functional alloys sintered in a normal-pressure hydrogen atmosphere. *Powder Technol.* 2024, 438, 119625. <https://doi.org/10.1016/j.powtec.2024.119625>
 30. Zhuang Z., Li Z. et al. The influence of ball milling conditions on the powder characteristics and sintering densification of MoCu alloy. *Int. J. Refract. Met. Hard Mater* 2024, 125, 106914. <https://doi.org/10.1016/j.ijrmhm.2024.106914>
 31. Dymek S., Lorent A., Wróbel M., Dollar A. Mechanical alloying and microstructure of a Nb–20% V–15% Al alloy. *Mater. Charact.* 47, 5, 2001, 375–381. [https://doi.org/10.1016/S1044-5803\(02\)00184-5](https://doi.org/10.1016/S1044-5803(02)00184-5)
 32. Kamil M.P., Sandyaning D., Wismogroho A.S., et al. Investigation of a Ni-38Mo binary alloy fabrication by mechanical alloying and spark plasma sintering. *Mater. Lett.* 2023, vol. 333, 133595, <https://doi.org/10.1016/j.matlet.2022.133595>
 33. Shi J., Lin Z., Liang Y., et al. Mechanical alloying of L21 phase Ni–Ti–Al alloy with high hardness: Influence of multiple process control agents. *Mater. Chem. Phys.* 2020, 256, 123728. <https://doi.org/10.1016/j.matchemphys.2020.123728>
 34. Rajath Hegde M. M., Pradeep N. B., et al. Synthesis and characterization of multi-walled carbon nanotube-reinforced Ti–Mg alloy prepared by mechanical alloying and microwave sintering. *J. Mater. Res. Technol.* 2024, 31, 1236–1249. <https://doi.org/10.1016/j.jmrt.2024.06.120>